

Emission of picosecond electromagnetic pulses from optically excited superconducting bridges

C. Jaekel, H. G. Roskos, and H. Kurz

Institut für Halbleitertechnik II, RWTH Aachen, Sommerfeldstrasse 24, D-52056 Aachen, Germany

(Received 2 April 1996; revised manuscript received 4 June 1996)

In this paper we examine the origin of the emission of picosecond electromagnetic pulses from current-biased superconducting bridges after optical excitation with femtosecond laser pulses. The peak frequency and the amplitude of the THz pulses are quantitatively correlated to the optically measured quasiparticle dynamics. We find that reflection and absorption within the superconductor fundamentally limit the ratio of the transmitted field amplitude to the generated signal to 10^{-3} . [S0163-1829(96)51534-1]

The discovery of high-temperature superconductors (HTS's) has renewed the interest in the physics of nonequilibrium superconductivity. From the point of view of applications, the pico- to subpicosecond relaxation back from nonequilibrium by recombination of the quasiparticles defines the principal frequency limit of devices based on the dynamical changes of Cooper-pair densities. All-optical measurements detecting the change of the optical properties after excitation with femtosecond laser pulses¹⁻⁶ have concentrated on the analysis of the quasiparticle dynamics. Time-resolved on- and off-chip voltage measurements have been applied to probe the electrical response of HTS's.⁷⁻⁹ The submillimeter-wave radiation emitted from an optically excited superconducting bridge can be detected¹⁰ by terahertz (THz) time-domain spectroscopy.^{11,12} In this paper, we present a study of THz emission from optically excited $\text{YBa}_2\text{Cu}_3\text{O}_{7-\delta}$ (YBCO) microbridges and relate the emission dynamics to the quasiparticle dynamics traced by all-optical reflection measurements.

The samples are homogeneous, fully *c*-axis-oriented YBCO films, deposited by dc sputtering on MgO substrates, with transition temperatures of 85 K. The film thickness has been chosen to be about 300 nm for the optical measurements to suppress multiple interference effects, and 70 nm for the THz-emission experiments to allow determination of the microwave conductivity.¹² Superconducting bridges, 50 μm wide and 50 μm long, are patterned by optical lithography and dry etching.¹³ After patterning they exhibit a transition temperature T_c of about 80 K. The bridges end in contacts that are tapered to suppress geometrical (antenna) resonances.

Reflectivity and transmission changes down to 10^{-7} are measured using a fast-scan pump-probe setup with 50 fs laser pulses from a 76-MHz-repetition-rate Ti:sapphire laser at a wavelength of 810 nm. The THz-emission experiments are performed in a nitrogen-flushed THz-spectroscopy setup. Coherent THz-radiation pulses are generated by excitation of a current-biased YBCO bridge with optical pulses. The laser focus on the bridge is 40 μm and the power of the laser beam is varied between 500 μW and 40 mW. The bias current is varied between 5 and 100 mA. Time-resolved detection of the generated THz pulses in the forward (transmission) and backward (reflection) direction is achieved with a 50 μm long photoconductive dipole antenna.¹⁴

The amplitudes of the Fourier transforms of the THz signals emitted in the forward direction are shown in Fig. 1 for different temperatures below T_c , obtained with a time-averaged laser power of $P_{\text{laser}} = 20$ mW and a bias current of 50 mA (time-domain data at 8 K: see inset). The amplitude

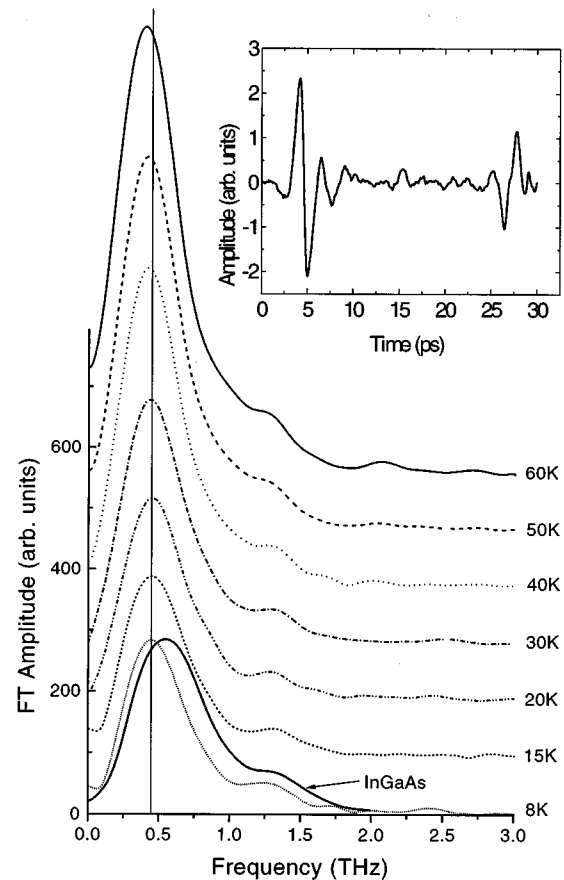


FIG. 1. Fourier transforms of the time-domain signals at different temperatures. For comparison, the emission spectrum of an InGaAs surface emitter normalized to the 8 K data is included. The inset shows a time-domain signal of the emitted pulse at 8 K. The second signal about 23 ps after the main transient is a substrate reflection of the emitted THz pulse. The weak oscillatory structure (also observed in the InGaAs transients) is due to absorption of the radiation by residual water vapor.

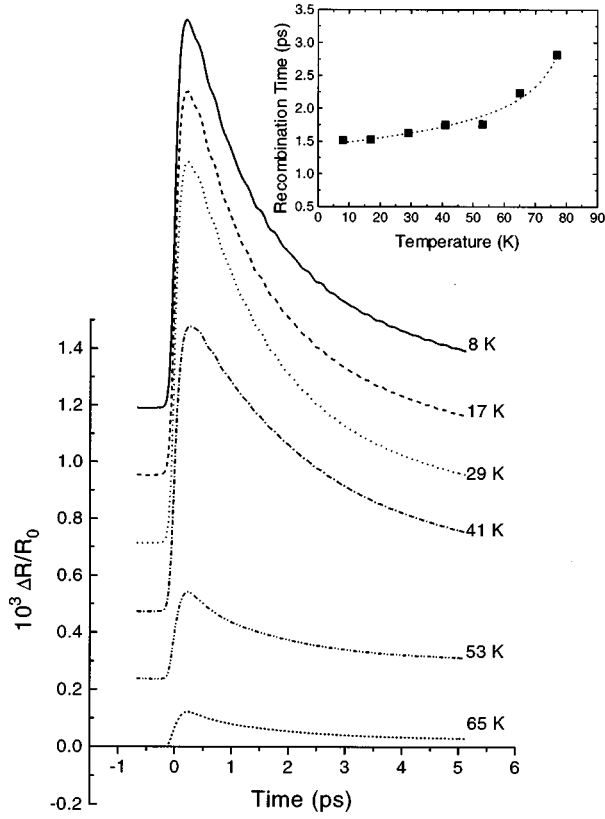


FIG. 2. Optical response of a YBCO thin film after excitation with fs laser pulses for several temperatures. The inset shows the quasiparticle recombination times derived by fits with Rothwarf-Taylor equations. The dashed line reproduces the dependence given in the text.

drops with falling temperature and the frequency shifts slightly to higher frequencies.

The amplitude is found to be proportional to the bias current as well as to the pump power (data not shown), proving the superradiant character of the emission.¹⁰ The amplitudes of the electrical fields detected in forward and backward direction have a ratio of $E_{\text{trans}}/E_{\text{ref}} \approx 2.1$. For comparison of the amplitudes of the radiated fields to that of a standard semiconductor surface emitter,¹⁵ an InGaAs wafer is measured in the same setup. At a laser power P_{laser} of 300 mW, the forward signal from the InGaAs sample is a factor of 5 higher than the field amplitude of the superconductor emission at 60 K, $P_{\text{laser}} = 20$ mW and a bias current of 50 mA.

In order to discuss the origin of THz emission from the superconducting bridge, we compare the THz results with the quasiparticle dynamics investigated by all-optical pump-probe reflection measurements. The time-resolved optical response of a YBCO film is shown in Fig. 2. The ultrafast rise of the reflectivity after excitation of the HTS at $t=0$ ps is attributed to Cooper pair breaking. The subsequent decrease of the reflectivity results from quasiparticle recombination.⁵ Except for $T \approx T_c$, the maximum density $\Delta N_{s,\text{max}}(T)$ of the optically broken Cooper pairs is small with respect to the overall density $N_s(T)$ of Cooper pairs in the Bose condensate. Assuming that the whole absorbed photon energy is used for breaking Cooper pairs and that there is an effective superconducting energy gap Δ_s , one estimates from the in-

cident optical power per pulse that $\Delta N_{s,\text{max}}(T)$ is on the order of 1% of the Cooper-pair density, for $T \ll T_c$. After the pair-breaking cascade, the maximum density of broken pairs is given approximately by $\Delta N_{s,\text{max}}(T) \approx E_{\text{photon}}/[2\Delta_s(T)]$, where E_{photon} is the energy density of the light absorbed in the superconductor. The time dependence of the reflectivity change $(\Delta R/R_0)(t)$ is expected to be directly proportional to the temporal evolution of the density $\Delta N_s(T, t)$ of the broken pairs:

$$\frac{\Delta R}{R_0}(T, t) = \frac{1}{R_0} \frac{\partial R}{\partial N_s} \Delta N_s(T, t). \quad (1)$$

$\Delta N_s(T, t)$ can be factorized as $\Delta N_s(T, t) = \Delta N_{s,\text{max}}(T) f_{N_s}(T, t)$, with a time-independent amplitude $\Delta N_{s,\text{max}}(T)$ and the normalized function $f_{N_s}(T, t)$ containing the full temporal evolution of the broken-pair density, respectively of the reflectivity change.

The dynamics of broken pairs can be modeled by Rothwarf-Taylor equations¹⁶ extended for the nonequilibrium case. The initial pair-breaking time is determined to increase from about 60 fs at $T \approx 0$ to about 120 fs at $T = 65$ K.¹⁷ The recombination time τ_r has a value of $\tau_0 = 1.5$ ps for $T \rightarrow 0$ with a temperature dependence given by $\tau_r = \tau_0 + 1.15 \tau_{e\text{-ph}}(T/T_c)/\sqrt{1 - T/T_c}$ (see inset of Fig. 2), where $\tau_{e\text{-ph}} = 385$ fs is a characteristic scattering time derived from BCS theory.¹⁸

For the interpretation of the THz emission, two aspects have to be considered. The first one is the generation of the electromagnetic pulse itself, the second one is the output coupling of the radiation from the superconducting film. We start with a description of the generation of the electromagnetic pulses. The electromagnetic response of the superconducting bridge can be understood from classical electrodynamics. Neglecting the normal-carrier contribution, the current density is given by $j_s = 2eN_s v_s$, where v_s is the velocity of the Cooper pairs. The first London equation and the condition of constant current yields¹⁹

$$E(T, t) = -j_s \frac{m_s}{4e^2 N_s^2(T)} \frac{\partial N_s(T, t)}{\partial t}, \quad (2)$$

where E is the electric field generated across the illuminated spot of the bridge and m_s is the mass of the superconducting carriers.

The electric field of the emitted THz pulse then depends on time and temperature according to

$$E(T, t) \sim \frac{1}{N_s^2(T)} \frac{\partial N_s(T, t)}{\partial t} \sim \frac{\Delta N_{s,\text{max}}(T)}{N_s^2(T)} \frac{\partial f_{N_s}(T, t)}{\partial t}. \quad (3)$$

According to Eqs. (3) and (1), the time dependence of the emitted THz field is proportional to the time derivative of the reflectivity change $(\Delta R/R_0)(T, t)$. Figure 3 displays the Fourier transforms of the time derivatives of these reflectivity changes. The transforms reveal a broad spectrum peaking at about 500 GHz and extending to more than 10 THz. The peaks in the region between 3 and 5 THz are due to phonons that are coherently excited by the femtosecond optical pulse.²⁰

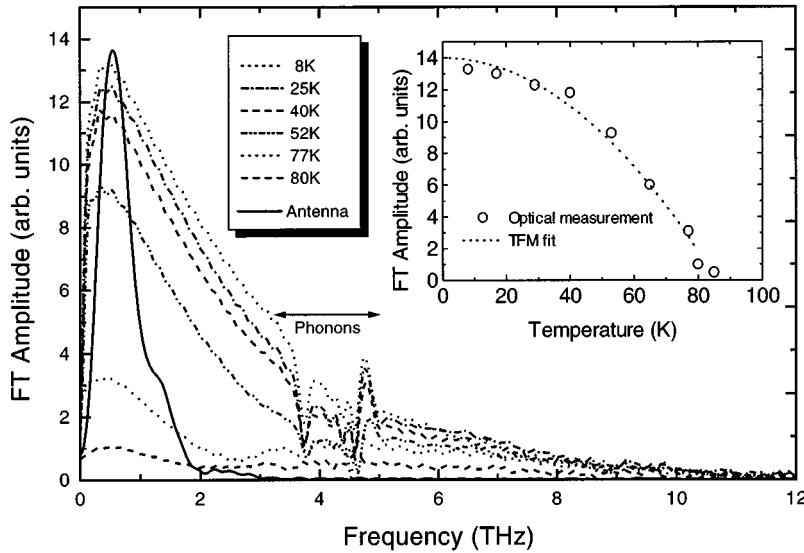


FIG. 3. Fourier transforms of the time derivative of the optical reflection measurements for several temperatures below T_c . The solid line shows the spectral sensitivity of the antenna determined with an InGaAs surface emitter. In the inset, the peak amplitudes after convolution with the antenna response are depicted.

Before analyzing the temperature dependence of the amplitudes, we first focus on the frequency of the main maximum, plotted in Fig. 4(a). With decreasing temperature, the peak frequency slightly shifts to higher frequencies. This behavior can be understood by the faster quasiparticle dynamics at low temperatures (see Fig. 2). In order to compare these results with the THz-emission experiments we must take the spectral response of the THz antenna into account (see solid line in Fig. 3). The response is measured with the InGaAs surface emitter that acts as a “white-light” source in the frequency range of interest. The full squares in Fig. 4 show the temperature dependence of the peak frequency after convolution with the antenna response function. The open circles and triangles represent the peak frequency obtained directly from the THz data of Fig. 1. In both cases, the peak frequency shifts towards higher values when the temperature falls. Except for a 5–10 % offset of the absolute values, there

is good agreement between the data sets. The backward-direction peak frequencies (circles) are offset relative to the forward-direction data (triangles). This shift is explained with typical variations in the alignment of the THz measurement setup. Given these variations, the agreement between the THz-emission data and the peak frequencies derived from the optical reflectivity measurements is fully acceptable.

Analyzing the amplitude of the THz-emission signal there is a profound difference in temperature dependence between THz amplitude and optical reflectivity changes. While the THz amplitude decreases with falling temperature, we find an increase of the maximum time derivative of the optical reflectivity change. This qualitative difference can be understood from Eq. (3), where the THz amplitude is found to be proportional to $\Delta N_{s,\max}(T)/N_s^2(T)$. $\Delta N_{s,\max}(T)$ depends inversely on the superconducting gap $\Delta_s(T)$. With falling tem-

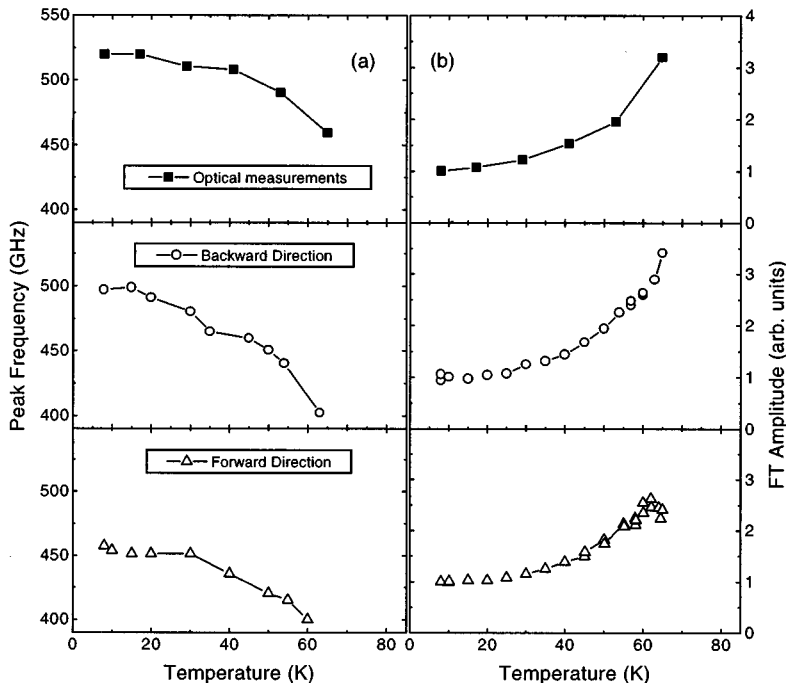


FIG. 4. Comparison of the temperature dependence of the peak frequency (a) and the signal amplitudes (b) as obtained from the THz measurements (circles and triangles) and from calculations with the data of the optical experiments (full squares).

perature, Δ_s increases, fewer Cooper pairs are broken, hence the emitted electric field E decreases. The same trend for E is found with respect to the Cooper-pair density $N_s(T)$.

For a correct evaluation of the THz-pulse emission, additionally output-coupling effects have to be taken into account. The electromagnetic pulse generated within the film is attenuated by absorption losses within the film and reflection losses at the film-air and at the film-substrate interface, respectively. The transmitted electric field is approximately described by the expression $E = E_0 t \exp(-\alpha d/2)$, d being the mean distance the pulse must travel, α the absorption coefficient, and t the transmission coefficient. The absorption coefficient is determined by the real part of the conductivity σ_1 and the reflection coefficient r via $\alpha = \sigma_1 / rc \epsilon_0$ with c being the speed of light in vacuum and ϵ_0 the permittivity of free space. The conductivity of the sample is directly determined by THz-transmission spectroscopy,¹² yielding absorption lengths of 35 nm at 65 K and 100 nm at 10 K for 0.5 THz. The transmission coefficients are given by $t = 2n_m / [n(T) + n_m]$ with $n(T)$ being the temperature-dependent index of refraction of the superconductor and n_m that of the interface medium ($n_{\text{vacuum}} = 1$, $n_{\text{MgO}} = 3.2$). $n(T)$ can be calculated with the general dependence $n(T) = c/\lambda(T)\omega$. $\lambda(T)$ is the penetration depth of the superconductor and is extracted from THz-transmission data of the thin films. We determine a penetration depth $\lambda(0 \text{ K})$ of 160 nm, yielding $n(0 \text{ K}) = 597$ at 0.5 THz and $T \rightarrow 0$. The temperature dependence of the penetration depth follows a two-fluid behavior. The very high value of $n(T)$ gives rise to a small transmission coefficient t of the order of 10^{-3} . The ratio of the calculated transmission coefficients at 70 K and at low temperature is $t(70 \text{ K})/t(0 \text{ K}) \approx 1.8$. For the difference between forward and backward measurements, we obtain a ratio of $t_{\text{trans}}/t_{\text{ref}} \approx 3.1$ explaining the higher amplitudes in forward direction.

With the time derivative of the relative reflectivity change determined directly from the experimental data, and with the model described above, the expected temperature dependence of the THz-field amplitude can be calculated. If we assume that the absorbed energy from the laser pulse does not change significantly with temperature for $T < T_c$, $\Delta N_{s,\text{max}}$ in Eq. 3 is reduced by a factor of $1/\Delta_s(T)$, where $\Delta_s(T)$ is assumed to be BCS-like [$\Delta_s(T) \sim \sqrt{1 - T/T_c}$]. The

temporal evolution of the gap parameter is neglected and N_s is assumed to be time independent because of the low density of broken Cooper pairs. The calculated THz-field amplitude is plotted in the upper part of Fig. 4(b) and compared in the lower part of the figure with the temperature dependence of the amplitudes of the THz signals. All data are normalized to the respective values for the lowest temperature. The lines in the figure are guides to the eye. The temperature dependences of the theoretically expected THz amplitude in the upper part of the figure and of the measured amplitudes displayed in the lower part are very similar for temperatures $T < 60 \text{ K}$. The deviations of the forward-radiation signal around 60 K result from a higher optical excitation power and a higher current density of $3 \times 10^6 \text{ A/cm}^2$ close to the critical current density chosen in these measurements. With these conditions, it is likely that all pairs are broken at $T \approx 60 \text{ K}$. We conclude that the temperature dependence of the strength of the THz radiation pulses from the superconducting bridge is determined by the thermal shrinkage of the superconductor energy gap and of the temperature dependent transmission and absorption coefficients.

With regard to practical applications, optically excited microbridges are to be compared with standard semiconductor surface emitters. The emission bandwidth is narrower than that of semiconductor surface emitters reflecting the slower dynamics of Cooper-pair breaking and quasiparticle recombination in relation to the instantaneous polarization and the carrier-transport dynamics of highly excited semiconductors. The emission efficiencies (ratio of emitted THz power to optical pump power) are roughly comparable. Although the current change in the bridge is fairly high, the emission efficiency is fundamentally limited by confinement of the radiation in the superconductor (high index of refraction by the supercurrent) and strong absorption (quasiparticles). Considering the need for patterning, sample cooling, and the limited long-term stability, superconductor bridges appear less attractive for the generation of general-purpose free-space radiation than for guided pulses in on-chip applications such as input ports of superconducting logic circuits.

We thank J. Hollkott and J. Auge for providing the samples. This work was supported by the German BMBF under Contract No. 13N6288.

¹J. Chwalek *et al.*, Appl. Phys. Lett. **57**, 1696 (1990).

²S. Han *et al.*, Phys. Rev. Lett. **65**, 2708 (1990).

³G. Eesley *et al.*, Phys. Rev. Lett. **65**, 3445 (1990).

⁴D. Reitze, A. Weiner, A. Inam, and S. Etamad, Phys. Rev. B **46**, 14 309 (1992).

⁵A. Frenkel, Phys. Rev. B **48**, 9717 (1993).

⁶C. Jaekel *et al.*, in *Proceedings of the European Conference on Applied Superconductivity* (Institute of Physics Publishing, Bristol, 1995), Vol. 2, p. 1103.

⁷F. Hegmann *et al.*, Appl. Phys. Lett. **67**, 285 (1995).

⁸N. Bluzer, Phys. Rev. B **44**, 10 222 (1991).

⁹A. Semenov *et al.*, Appl. Phys. Lett. **60**, 903 (1992).

¹⁰ Similar THz measurements as those reported here have been performed by M. Hangyo *et al.* (unpublished).

¹¹M. Nuss *et al.*, Phys. Rev. Lett. **66**, 3305 (1991).

¹²C. Jaekel *et al.*, Appl. Phys. Lett. **64**, 3326 (1994).

¹³R. Barth *et al.*, Appl. Phys. Lett. **63**, 1149 (1993).

¹⁴P. Smith, D. Auston, and M. Nuss, IEEE J. Quantum Electron. **QE-24**, 255 (1988).

¹⁵X.-C. Zhang and Y. Jin, in *Perspectives in Optoelectronics*, edited by S. Iha (World Scientific, Singapore, 1995), Chap. 3.

¹⁶A. Rothwarf and B. Taylor, Phys. Rev. Lett. **19**, 3038 (1967).

¹⁷C. Jaekel, M. Schröer, H. Roskos, and H. Kurz (unpublished).

¹⁸A. Kadin and A. Goldman, in *Nonequilibrium Superconductivity*, edited by D. Langenberg and A. Larkin (North-Holland, Amsterdam, 1986), Chap. 7.

¹⁹F. A. Hegmann and J. S. Preston, Phys. Rev. B **48**, 16 023 (1993).

²⁰W. Albrecht, T. Kruse, and H. Kurz, Phys. Rev. Lett. **69**, 1451 (1992).